Spatial Patterns of Tree-Growth Anomalies in the United States and Southeastern Canada*

DAVID MEKO

Laboratory of Tree-Ring Research, University of Arizona, Tucson, Arizona

EDWARD R. COOK

Lamont-Doherty Earth Observatory, Palisades, New York

DAVID W. STAHLE

Department of Geography, University of Arkansas, Fayetteville, Arkansas

CHARLES W. STOCKTON AND MALCOLM K. HUGHES

Laboratory of Tree-Ring Research, University of Arizona, Tucson, Arizona

(Manuscript received 7 July 1992, in final form 24 February 1993)

ABSTRACT

A network of 248 tree-ring chronologies in the conterminous United States is assembled and analyzed by rotated principal components analysis (RPCA) to delineate "regions" of common tree-growth variation during the period 1705–1979. Spatial continuity of the tree-ring data is summarized by variogram analysis, and tree-ring data are gridded before RPCA to reduce effects of site clustering. Principal component drought information is evaluated by comparing PC scores and primary pattern coefficients with Palmer Drought Severity Index (PDSI) data from instrumental records.

High PC pattern coefficients group geographically into regions coinciding roughly with nine drought regions delineated by RPCA of PDSI by other researchers. The drought signal as measured by the correlation between tree-ring PC scores and July PDSI, 1929–79, is strongest in the South and the interior West ($r > 0.7$), and weakest in the Northeast and Pacific Northwest ($r < 0.16$). A count of years with large negative PC scores in multiple regions marks the 1950s as the extreme in widespread drought across the southern United States to 1705.

Tree-growth regions are sensitive to whether tree-ring data are gridded before RPCA. Principal components on ungridded tree-ring data tend to center on dense clusters of sites. The importance of site density is most noticeable in the RPCA results for the southeast, where the gridded data yield a PC centered on a group of climate-sensitive but widely spaced bald cypress chronologies. Cross-validation indicates that gridding of tree-ring anomalies over different species for drought reconstruction is more appropriate in the semiarid southwest than in cooler, moister regions—especially the northeast and the Pacific Northwest. Our results endorse the large-scale chronology network as a long-term proxy for the spatial and temporal patterns of past drought across the United States.

1. Introduction

Networks of tree-ring chronologies were first applied in climatology by Fritts (1965) to infer spatial patterns of moisture conditions from contoured maps of growth anomalies at tree-ring sites in western North America. Multivariate regression methods later allowed extension of climatological inferences to the eastern United States from sites concentrated west of the plains (Fritts et al. 1979; Fritts 1991). Field collections east of the Rocky Mountains have since given a regionally balanced tree-ring coverage with which to examine continental patterns of climate anomalies. These collections until now have been applied only to regional-scale climate reconstructions (e.g., Cleaveland and Duvick 1992; Stockton and Meko 1983; Stahle and Cleaveland 1992; Cook et al. 1992). The collections could improve the accuracy of large-scale climate reconstructions and facilitate studies of species dependence in the response of tree-growth to climate change. Understanding the covariance structure of growth anomalies on the continental scale is an important step in climatological application of these data.

In this paper, we apply rotated principal components analysis (RPCA) to an expanded tree-ring network to identify spatial modes of tree-ring variations over the

* Lamont–Doherty Earth Observatory Contribution Number 5041.

Corresponding author address: Dr. David Meko, Laboratory of Tree-Ring Research, Bldg. #58, University of Arizona, Tucson, AZ 85721.

conterminous United States. We address effects of species differences and sample distribution to the principal components (PC), and compare PC scores and pattern coefficients with climatological data to evaluate usefulness of the network for drought studies.

2. Data

Site chronologies, each consisting of ring width indices averaged over many trees, were obtained from tree-ring laboratories at the University of Arizona, University of Arkansas, and Lamont-Doherty Earth Observatory of Columbia University. Additional chronologies not yet archived in laboratory databases were contributed by individual researchers (see Acknowledgments). The network comprises 248 chronologies screened from more than 600 on criteria of time coverage and likely sensitivity to drought. Upper tree-line bristlecone pine (*pinus aristata*) and other species with a climate signal not clearly related to drought are excluded. The network covers the time period 1700–1979, and includes 26 species, 9 of which are represented by 10 or more chronologies (Figs. 1 and 2, Table 1).

The network samples all major climatic provinces of the United States except the Gulf Coast and the High Plains. Sites cluster densely in parts of the Sierra Nevada, the Southern Rockies, and the Colorado Front Range (Fig. 1). Gaps in spatial coverage result from a lack of suitably old and datable trees and from the rejection of chronologies without complete data for the period 1700–1979. The gap centered on the Utah–Colorado border, for example, could have been avoided by including sites collected in the 1960s and 1970s.

Climate data used are monthly Palmer Drought Severity Indices (PDSI), 1929–1988, for 1035 stations in the National Drought Atlas network (Willeke et al. 1991). The PDSI had been recalculated by Willeke et al. (1991) using precipitation and temperature data from the Historical Climate Network (Karl et al. 1990).

a. Variance stabilization and prewhitening

Ring widths had previously been standardized into "site chronologies," indices of annual growth departures comparable from site to site (Fritts 1976; Cook et al. 1990). The raw data for a chronology are time series of measured ring widths of cores taken from several trees at a site. Standardization includes 1) detrending core ring widths to remove low-frequency variability caused by aging of the tree, changes in competition, and other nonclimatic influences, and 2) averaging the detrended core ring widths to reduce nonclimatic noise specific to individual trees. Core indices were computed as a ratio of measured ring width to a statistically fitted trend line. The form of trend line varies from one chronology to another, depending mainly on site type. Ring widths from open-growth sites with little competition among trees for moisture and light were typically detrended with a straight line

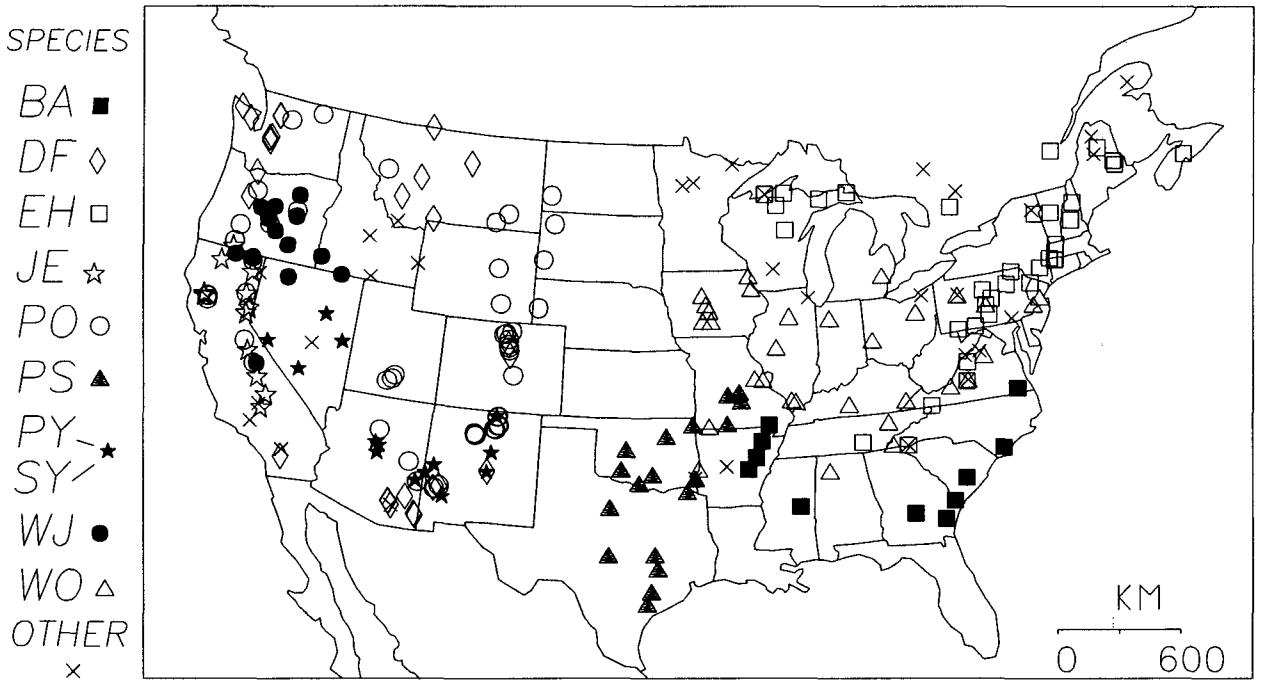

FIG. 1. Map showing locations of tree-ring sites, coded by species. The nine species with the most sites are marked by unique symbols, keyed at left and defined in Table 1. Other species are marked by "X."

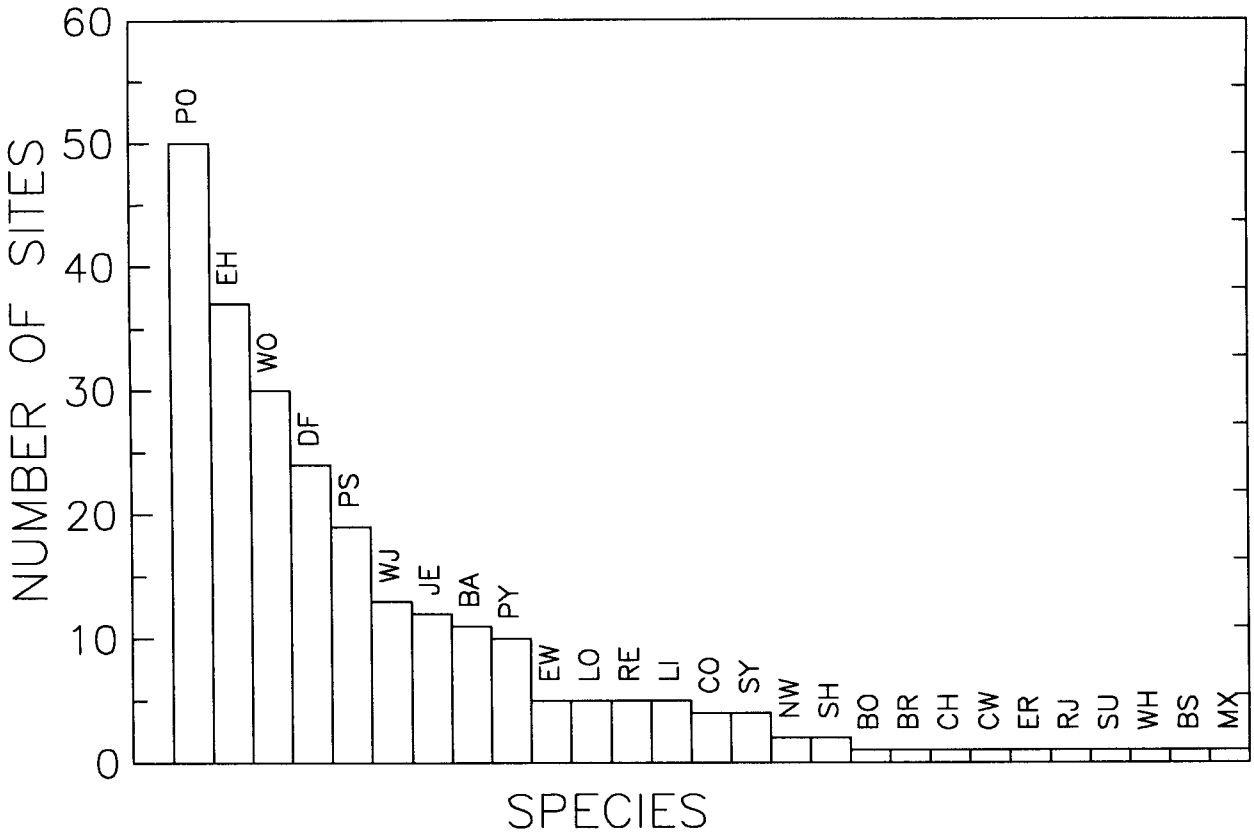

FIG. 2. Histogram of the number of tree-ring sites by species. Species codes are defined in Table 1.

TABLE 1. Key to species.

Abbreviation	Species
BA	Bald cypress—taxodium distichum
BO	Bur oak—quercus macrocarpa
BR	Bristlecone pine—pinus aristata
BS	Big-cone spruce—pseudotsuga macrocarpa
CH	Carolina hemlock—tsuga caroliniana
CO	Chestnut oak—Quercus montana
CW	California white oak—quercus lobata
DF	Douglas fir—pseudotsuga menziesii
EH	Eastern hemlock—tsuga canadensis
ER	Eastern red cedar—juniperus virginiana
EW	Eastern white pine—pinus strobus
JE	Jeffrey pine—pinus jeffreyi
LI	Limber pine—pinus flexilis
LO	Lodgepole pine—pinus contorta
MX	Mixture of species
NW	Northern white cedar—thuja occidentalis
PS	Post oak—quercus stellata
PO	Ponderosa pine—pinus ponderosa
PY	Pinyon pine—pinus edulis
RE	Red pine—pinus resinosa
RJ	Rocky Mountain juniper—juniperus scopulorum
SH	Shortleaf pine—pinus echinata
SY	Singleleaf pinyon—pinus monophylla
SU	Sugar pine—pinus lambertiana
WH	White pine—pinus strobiformis
WJ	Western juniper—juniperus occidentalis
WO	White oak—quercus alba

or modified negative exponential curve (Fritts et al. 1976); ring widths from other site types were typically detrended with a cubic spline (Cook and Peters 1981). A goal in detrending is to avoid as much as possible the removal of low-frequency variance that might be climatic in origin. Straight-line and negative-exponential methods are conservative in removing only monotonic trend. Cubic splines can remove higher-frequency fluctuations, but the frequency response of the spline can be specified such that the limitation on resolvable climate frequencies is known (Cook and Peters 1981).

Site chronologies were adjusted by variance stabilization and autoregressive filtering to reduce distortion of spatial growth patterns from nonclimatic sources. Variance was stabilized because not all chronologies had been developed following guidelines to guard against spurious variance trends caused by such factors as changing sample size (Wigley et al. 1984) and species-dependent changes in the earlywood–latewood proportions in the ring (Shiyatov et al. 1990). We uniformly stabilized the variance in each chronology by removing monotonic trends in the absolute departures from the mean for the 1700–1979 common period by a method included as an option in the tree-ring standardization program AutoRegressive Standardization ARSTAN (Cook and Holmes 1984). Mathematics are

given in the Appendix. Absolute values of the annual departures from the 1700–1979 mean are first fit to a straight line or modified negative exponential curve. The annual departures are then scaled by the ratio of the 1700–1979 mean absolute departure to the value of the fitted curve in each year. Because of this adjustment, the data cannot be used to test for monotonic trend in climate variance over 1700–1979.

After variance stabilization, the chronologies are still unsuitable for identification of spatial modes of annual growth anomalies because of site to site differences in autocorrelation. Autocorrelation in tree-ring indices is partly biological in origin and varies greatly from site to site (Fritts 1976). A map of annual growth departures over a network of chronologies comprising many different species and site types therefore reflects a mix of current and past years' environmental conditions. To amplify the contemporaneous signal in the tree-ring network, variance-stabilized chronologies were prewhitened using low-order autoregressive (AR) models. The prewhitening model is

$$x_t = \phi_1 x_{t-1} + \cdots + \phi_p x_{t-p} + e_t \qquad (1)$$

where x_t is the tree-ring index in year t after stabilizing variance and subtracting the 1700–1979 mean, p is the order of the model, $\phi_1, \ldots, \phi_p$ are the AR parameters, and e_t is the AR residual, or the prewhitened tree-ring index. The best-fit model up to order $p = 5$ for each chronology was selected by the Akaike Information Criteria (AIC) (Salas et al. 1980). Autocorrelation in many chronologies is more complex than can be explained by a first-order autoregressive model. The most common model fit was second order (96 sites), followed by first order (80 sites). One chronology required a fifth-order AR model. Examination of time series plots of AR residuals from competing models with similar AIC values showed that the effect on e_t of possible overfitting of AR models by the AIC (Katz 1982) is of little practical importance.

The percentage of variance explained (VE) by the fitted AR models ranges from less than 1% for a pinyon pine site in Arizona to more than 65% for a ponderosa pine site in Washington. The percentage of variance of explained is between 5% and 25% for more than half the chronologies. Differences in autocorrelation depend strongly on species: median VE ranges from 5.5% for bald cypress to 30.6% for eastern hemlock.

Subsequent analyses use the prewhitened, variance-stabilized series, with original chronology means restored:

$$Z_{t,j} = e_{t,j} + \bar{X}_j, \quad t = 1,275 \quad j = 1,248, \qquad (2)$$

where $e_{t,j}$ is the AR residual series for the jth chronology, and $\bar{X}_j$ is the corresponding chronology mean. The year index t covers the years 1705–1979 instead of 1700–1979 because up to five initial years are lost in prewhitening.

b. Spatial continuity and gridding

To avoid biasing of PCs by the uneven spatial distribution of samples (Kutzbach and Guetter 1980; Karl et al. 1982), the tree-ring series Z was gridded before RPCA. Grid design was guided by a variogram analysis of spatial continuity (Isaaks and Srivastava 1989). Variogram analysis, a geostatistical method that has been applied in climatology by Finkelstein (1984) and Bigg (1991) and in dendroclimatology by Chbouki (1991) and Shao (1992), can treat the spatial continuity for each map or year individually. This approach is useful for quantifying continuity differences related to type of climate anomaly—for example, differences in the spatial scale of precipitation and streamflow anomalies between drought years and wet years (Julian 1970; Langbein and Slack 1982).

The diagnostic tool in variogram analysis is the variogram (or semivariogram), a plot of half the average squared difference between paired data values against separation distance. The variogram for geophysical data typically increases from a low value near zero separation distance to a uniformly high value at some distance called the range, where the effect of small-scale correlation is diminished. The theoretical value of the variogram at zero separation distance is the nugget, and the value reached or asymptotically approached at the range is the sill (Isaaks and Srivastava 1989). The range of a variogram for a map of annual tree-ring indices depends on the size of the regions of high and low growth. If regions of high and low growth are localized, the range is small. If a map is dominated by large-scale patterns—for example, a gradient from high growth in the east to low growth in the west—the range might

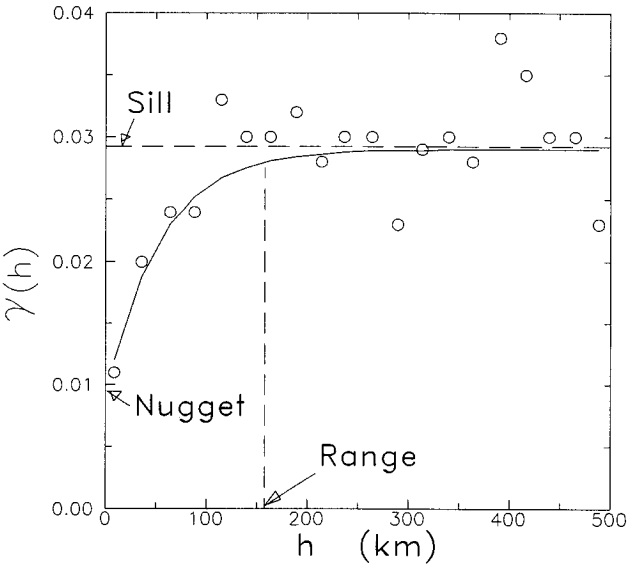

FIG. 3. Sample and model variogram of tree-ring index for year 1958.

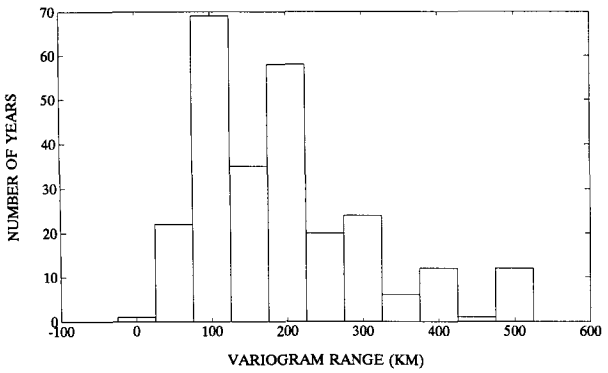

FIG. 4. Histogram of ranges for variograms for years 1705–1979. A range greater than 500 km was set to 500 km for the tabulation. Fifteen years whose variograms were erratic in shape were excluded from the analysis.

be larger than the search radius used for computing the variogram.

Omnidirectional variograms were computed for each of the 275 tree-ring maps from 1705–1979 using the Geostatistical Environmental Assessment Software (GEO-EAS) statistical package (Englund and Sparks 1990). Sample sizes in individual distance classes were too small to allow evaluation of directional effects. The variogram was computed to a maximum separation distance of 500 km. The 0–500-km range was divided into 20 approximately equally spaced distance classes for the computations. The variogram for each year was fit to a Gaussian, exponential, or linear model by a trial-and-error visual curve fitting procedure described by Englund and Sparks (1990).

The increase of the variogram with separation distance of sample points is illustrated by the tree-ring variogram for 1958 (Fig. 3). The sharp increase over the first 100–300 km is typical of sample variograms for many years. This variogram fit an exponential model (Isaaks and Srivastava 1989) with selected values of 160 km for the range, 0.009 for the nugget, and 0.020 for the sill. Sample variograms for most years contained much more scatter than the example in Fig. 3. Twelve sample variograms did not reach a plateau within the maximum 500-km separation distance used to compute the variogram, and 15 were too irregular in shape for identification of the range. A histogram of ranges for variograms reaching a plateau indicates that a range of 300 km or less is representative of most years (Fig. 4). This result is consistent with Cropper and Fritts's (1982) finding of high, positive, time-series correlation between tree-ring chronologies in western North America to a separation distance of about 250 km.

The increase of the tree-ring variograms with separation distance suggests that grid weights should be a function of distance from grid points. Inverse-distance weighting (IDW) was selected because variogram shapes varied too much from year to year to justify a more complicated weighting function. Grid spacing for IDW was set to 300 km, the separation distance over which the tree-ring variograms generally increase most steeply. The search distance was set to 213 km, the shortest distance ensuring that all tree-ring sites between grid points enter the analysis. A threshold minimum distance of 30 km was arbitrarily set in the gridding algorithm to avoid assigning unreasonably high weights to sites close to grid points.

The weighting algorithm for a grid point is

$$Z^* = \left(\sum_{i=1}^{p} \frac{Z_i}{d_i}\right) \Big/ \left(\sum_{i=1}^{p} \frac{1}{d_i}\right) \qquad (3)$$

where p is the number of sites within the search radius, Z_i is the tree-ring index at the ith chronology, and d_i is the greater of 30 km and the distance from the ith site to the grid point. The resulting grid has 89 grid points (Fig. 5). Each gridded value is a weighted average of between 1 and 14 individual series ($1 \leqslant p \leqslant 14$). Gaps in the grid are found where no tree-ring sites are within 213 km of a grid point. Largest gaps are in the High Plains and along the Gulf Coast.

Gridding was cross-validated by checking the ability of algorithm (3) to reproduce the tree-ring data at the individual sites. Cross-validation by this method was possible for only 237 tree-ring sites—those with at least one other site within the 213-km gridding search radius. A sample (tree-ring chronology) was temporarily discarded from the dataset, and the discarded sample value was estimated by (3). The procedure was repeated for all sample points and years. The accuracy of estimation was measured by the correlation coefficient between the observed and estimated tree-ring series for 1705–1979. A map showing the distribution of correlation coefficients indicates that gridding cross-validates best in the Southwest, and worst in the Pacific Northwest and New England (Fig. 6). Twelve of 13 sites with correlations greater than 0.85 are in Arizona and New Mexico. Correlation is significantly greater than zero at the 99% confidence level ($r > 0.15$) for 233 of 237 sites, and scattered high correlations ($r > 0.7$) can be found in most regions. Where correlations are low, as marked by small circles in Fig. 6, gridding is most likely to obscure important site-to-site differences in growth responses to climate. Because the "true" and estimated series are at the site locations, not the grid points, this exercise only indirectly cross-validates gridding. The suitability of gridded values for representing tree-growth anomalies is especially uncertain along the edges of the grid, where information has a directional bias and the number of sites in the search radius is often small.

3. Spatial modes of growth variations

a. Rotated principal components analysis (RPCA)

Principal components were extracted from the correlation matrix of the gridded tree-ring data Z^* in an

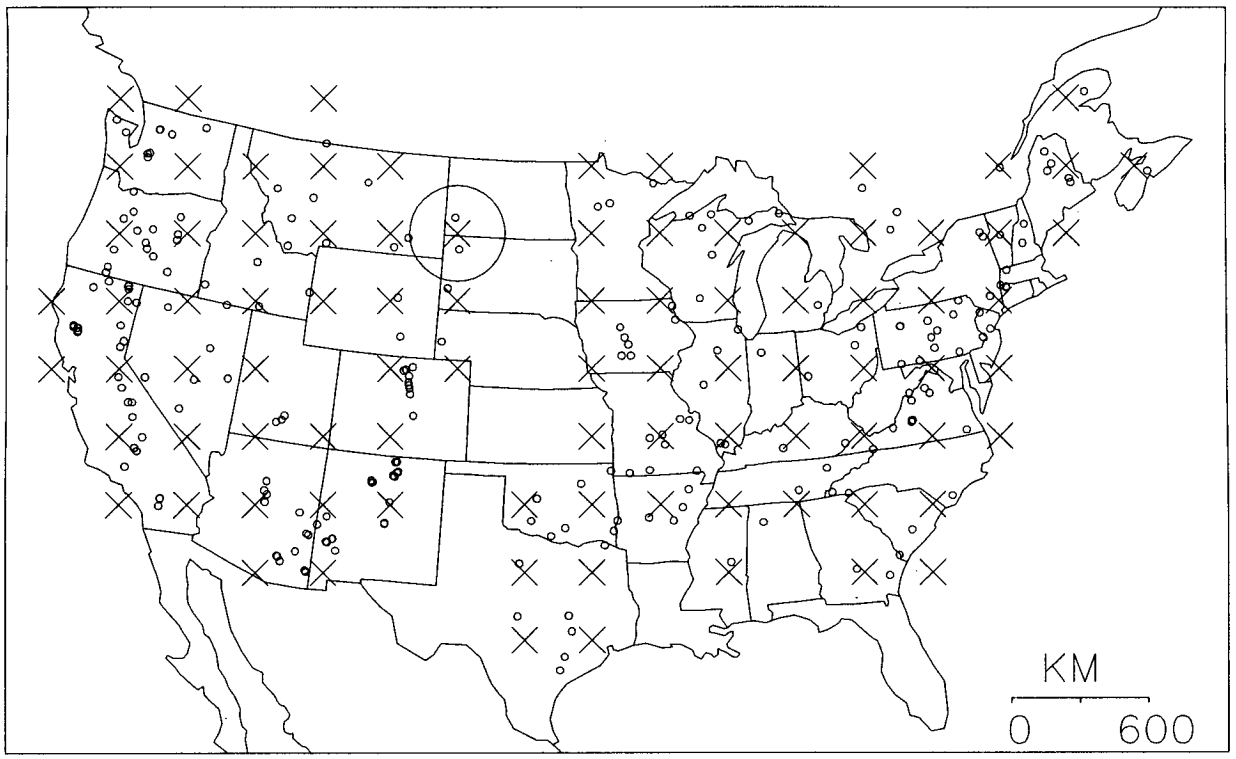

FIG. 5. Map showing locations of 89 grid points used in developing gridded version of tree-ring index. Tree-ring sites are marked by small circles. The search radius for gridding is shown by the large circle in North Dakota.

S-mode principal components analysis (PCA) to identify subgroups of grid points that covary similarly over the period 1705–1979. The mathematical model for PCA and the application of *S* mode PCA to the regionalization of climatological and meteorological data are described by Richman (1986). The "variables" index in this application refers to the 89 grid points, and the "individuals" index to the 275 years. The PCA was done on the correlation matrix because variance at a grid point depends on the number of chronologies in the search radius.

The percentage of variance explained by the unrotated PCs drops sharply over the first 13 PCs—from 13.3% for PC1 to less than 2% for PC13 (Fig. 7). Twenty-two PCs have eigenvalues greater than 1; these PCs account for a cumulative 76% of the variance. The loadings maps for the unrotated PCs (not shown) are not discussed here except to note that the patterns for the first few PCs strongly resemble generic patterns typically associated with domain shape dependence (Richman 1986). Such patterns are generally inferior to those from RPCA for depicting individual modes of variation in data (Richman 1986).

Principal components were rotated by the direct oblimin method, which attempts to minimize the simplicity criterion

$$F(P) = \sum_{p<q=1}^{m} \left(\sum_{j=1}^{n} b_{jp}^2 b_{jq}^2 - \frac{\delta}{n} \sum_{j=1}^{n} b_{jp}^2 \sum_{j=1}^{n} b_{jq}^2 \right) \quad (4)$$

where P is the primary pattern matrix with elements b_{jp}, m is the number of PCs rotated, n is the number of variables (grid points), and δ is a parameter controlling the obliqueness of the rotation (Jennrich and Sampson 1966). The parameter δ was set to zero, specifying the direct quartimin method of rotation (Harman 1967, p. 335). This method emphasizes simplifying the rows of P, such that under simple structure a grid point has low coefficients on most PCs, and high coefficients on one or a few PCs.

The number of PCs rotated was set to nine to facilitate comparison of tree-ring regions with drought regions identified by Karl and Koscielny (1982) in an RPCA of PDSI data. Nine PCs explain 55% of the variance of the gridded data, and encompass the steepest part of the curve of fractional variance explained against unrotated mode number (Fig. 7).

The spatial coherence in the mapped PC pattern coefficients suggests that the tree-growth patterns are governed by large-scale environmental influences (Fig. 8). High coefficients cluster into regions as follows: PC 1, 2, and 3 as ranked in importance by the sum of squares of the coefficients are centered on Arizona, New England, and the upper Midwest. Principal components 4, 5, and 6 are centered on northern California, Montana, and Arkansas. Principal components 7, 8, and 9 are centered on Texas, Washington, and Georgia. Comparison of pairwise plots of pattern coefficients with idealized plots in Richman (1986) indicates that

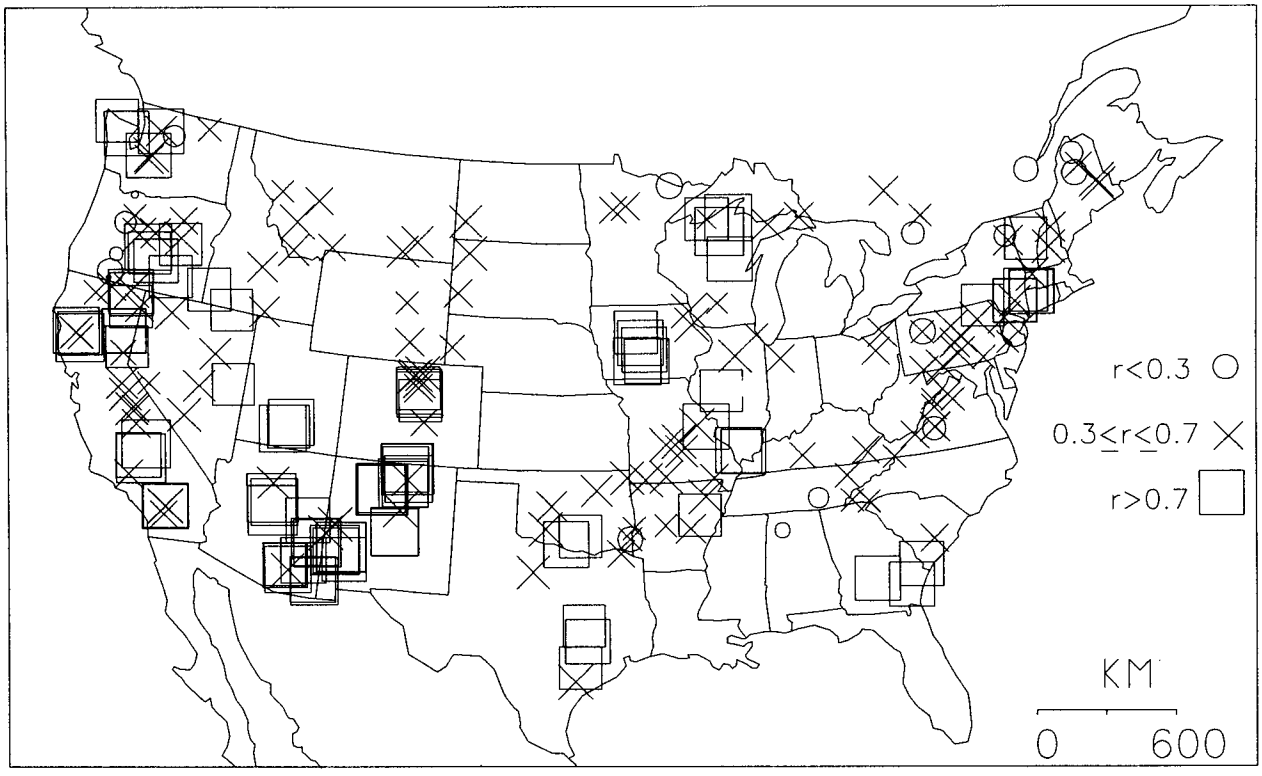

FIG. 6. Map summarizing results of cross-validation of tree-ring gridding. Each symbol represents the product–moment correlation coefficient, 1705–1979, between the observed tree-ring index at a site and the tree-ring index estimated by gridding. Symbol type and size are determined by the value of the correlation coefficient. The largest square corresponds to a correlation of 0.91 for a ponderosa pine site in western New Mexico. The smallest circle corresponds to a correlation of −0.10 for a Jeffrey pine site in southwestern Oregon.

the structure in the rotated tree-ring PCs is weak simple to strong simple. An example of weak simple structure is shown in the pairwise plot for PCs 1 and 7, representing adjacent regions centered on Arizona and Texas (Fig. 9). Grid points with high coefficients on both PCs have been numbered in the plot. The corresponding pair of pattern-coefficient maps shows that these grid points are located in Arizona, New Mexico, and southern Colorado (Fig. 8). In contrast, the maps for PCs 1 and 8 (Arizona and Washington) show strong simple structure: grid points with high coefficients on one PC have low coefficients on the other. The departure from strong simple structure in PC pairs from adjacent regions (e.g., PCs 1 and 7) is characteristic of the data, and is expected because the climate anomalies influencing tree growth (e.g., seasonal precipitation and temperature anomalies) are not strictly confined within regional boundaries. Intermediate grid points might fall at some times under the climate anomalies associated most strongly with one region, and at other times under those associated with the adjacent region.

b. *Effect of rotation*

Oblique rotation was preferred to orthogonal rotation because there is no reason to expect patterns of tree-growth anomalies to be orthogonal. Nevertheless, we found no appreciable difference between the pattern coefficient maps of Fig. 8 and maps of loadings from varimax rotation (not shown). Karl and Koscielny (1982) similarly reported little difference in PCs of historical Palmer Drought Index by varimax and oblique rotation. The PC scores from oblique rotation are only weakly intercorrelated: the highest product–moment correlation is 0.23 between PC2 and PC3. For normally

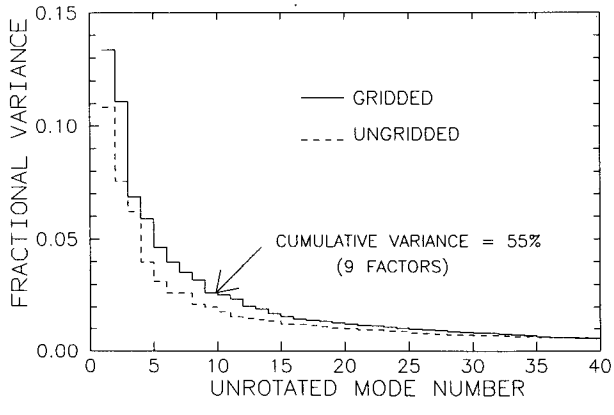

FIG. 7. Plot of fractional variance explained against component number for unrotated PCs from PCA of gridded and ungridded tree-ring index.

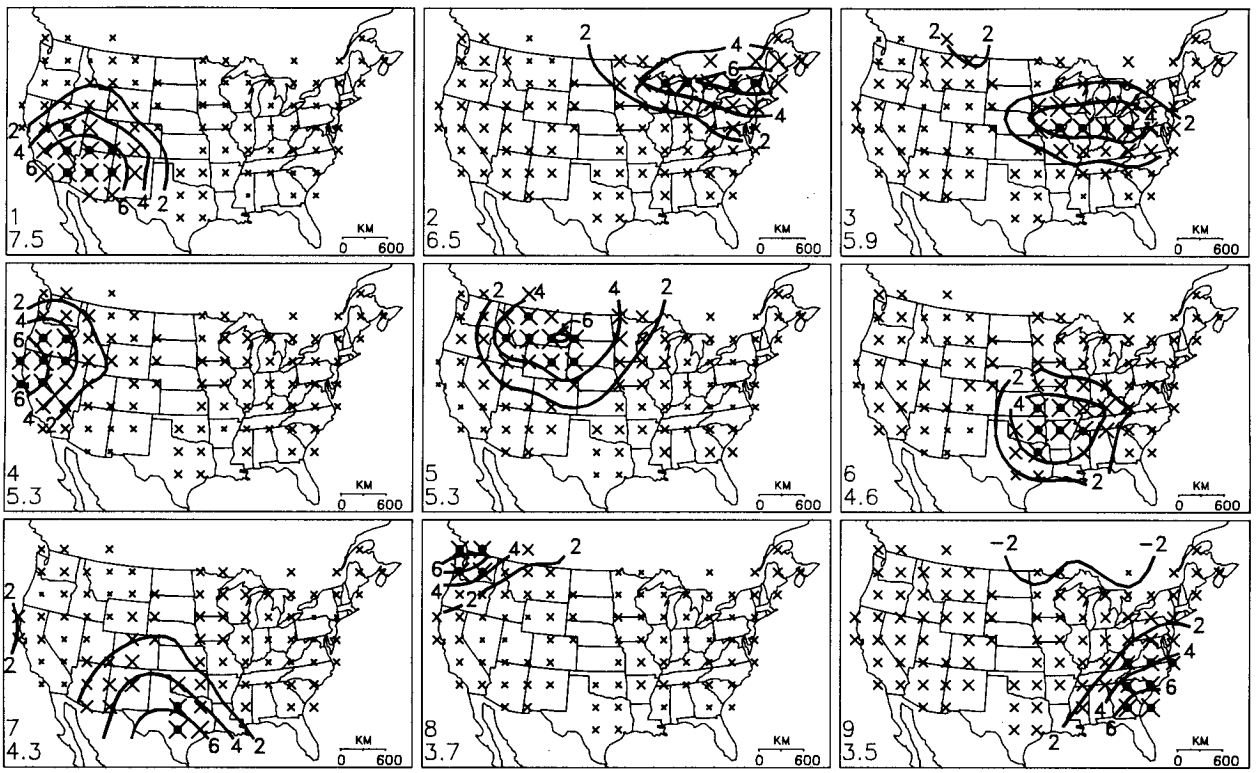

FIG. 8. Maps of primary pattern coefficients for nine obliquely rotated PCs of gridded tree-ring indices. Symbols are scaled such that the diameter for the largest coefficient is four times that for the smallest coefficient. PC number and sum of squares of coefficients are listed at lower left.

distributed and uncorrelated populations, this correlation is significant at the 99% level (Panofsky and Brier 1968), but indicates little variance in common.

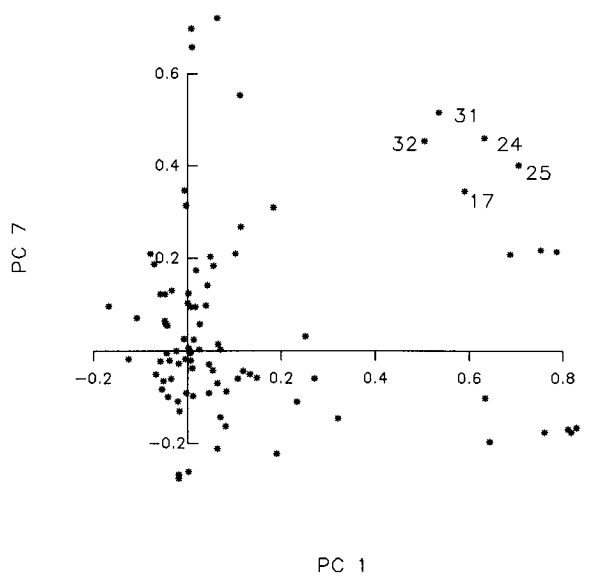

FIG. 9. Pairwise plot of primary pattern coefficients for rotated PCs centered on Texas (PC7) and Arizona (PC1). Five grid points with high coefficients on both PCs are numbered. These grid points are in southern Arizona, eastern New Mexico, and southern Colorado (Fig. 8).

Rotation of only nine PCs discards 45% of the variance of the gridded tree-ring data as noise. Rotation of more PCs using an objective cutoff criterion (e.g., an eigenvalue of 1) would be appropriate for studying smaller-scale aspects of tree-growth patterns. Nine is probably not the best number of PCs to rotate even for summarizing large-scale patterns because PC9 is on a "shelf" in the variance-explained plot (Fig. 7). One fewer or two more PCs might be rotated under the variation of the "scree test" criterion recommended by O'Lenic and Livezey (1988). We found that rotation of more than nine PCs fragmented the patterns in Fig. 8 into subregions. As the number of components rotated approached the number of grid points, the "regions" became isolated grid points or small groups of points, and the PC scores became highly intercorrelated. The maximum correlation between PC scores rose to 0.35 when 22 PCs were rotated, and to 0.65 when 75 PCs were rotated.

c. *Effect of gridding*

Cross-validation of gridding, as discussed previously, indicates that gridded tree-ring data are poorly representative of growth variations at some sites, especially in the Pacific Northwest and New England. We evaluated the effect of gridding on the identified growth patterns by repeating the RPCA using the ungridded tree-ring series. The percentage of variance accounted

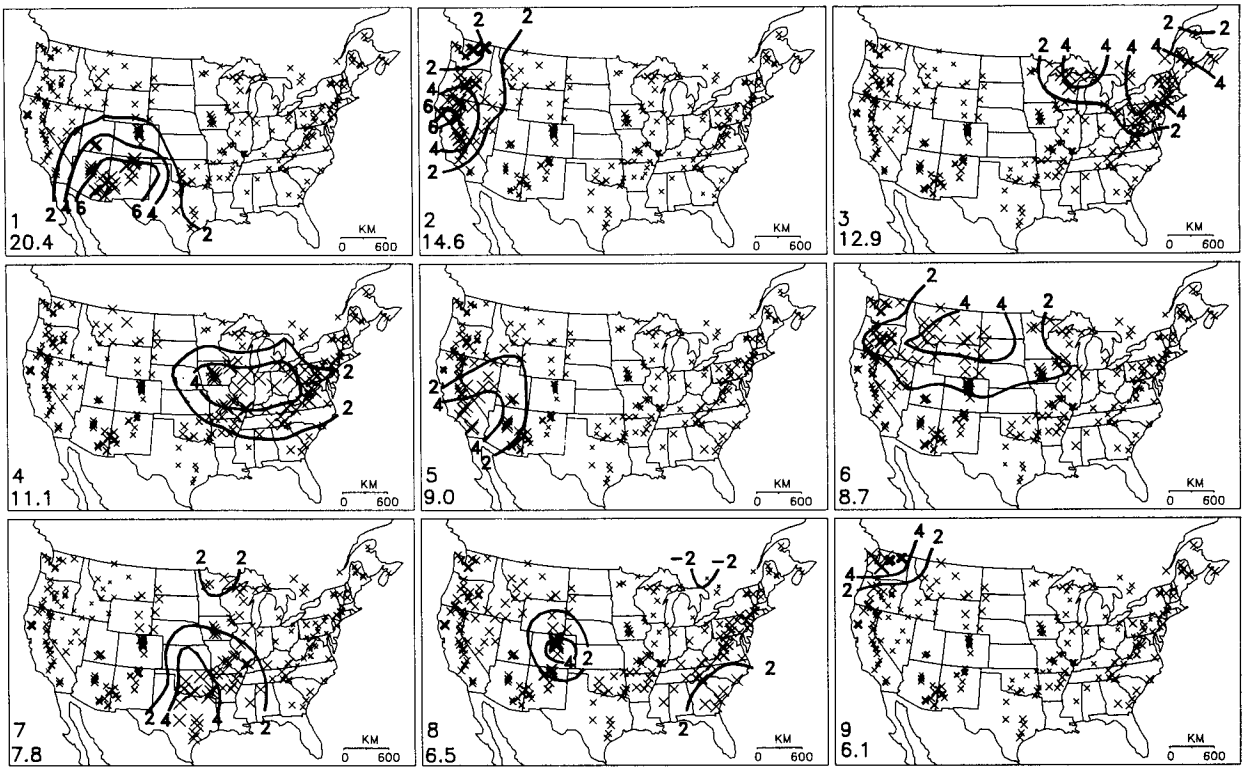

FIG. 10. Maps of primary pattern coefficients for nine obliquely rotated PCs of ungridded tree-ring indices. Two bold symbols in Washington mark ponderosa pine sites whose large pattern coefficients suggest species dependence in PCs (see text). Remainder of caption as in Fig. 8.

for by the first nine PCs ranges from 11% to 2% (Fig. 7). Nine components account for 41% of the variance, compared with 55% for the gridded data.

The nine rotated PCs of the ungridded data (Fig. 10) differ considerably from those of the gridded data (Fig. 8) in the geographical distribution of high and low pattern coefficients. An important difference probably related to site density is that no PC for the ungridded data centers on the southeast. Bald cypress, the dominant tree-ring species in the southeastern part of the network, has a strong seasonal precipitation signal (Stahle and Cleaveland 1992), but the sites are much more widely spaced than in other parts of the network (Fig. 1). Gridding apparently benefits the RPCA by amplifying the importance of the few widely spaced but climate-sensitive bald cypress sites in the southeast to the total variance of the tree-ring data.

The clusters of high and low PC pattern coefficients for the ungridded data group geographically and cross species boundaries, implying that large-scale environmental influences override species influences on growth departures. Species differences are least important to the PC pattern coefficients in the Southwest: coefficients on ungridded PC1 are uniformly high on many chronologies from three different conifer species (Fig. 1 and Fig. 10). Species differences are more important in other regions. For example, two ponderosa pine sites in Washington have small coefficients on PC9—centered on Washington—and high coefficients on PC2, centered far away in northern California (see darkened symbols on Fig. 10). All other chronologies in the core region for PC9 are Douglas fir. The same two ponderosa pine sites also had poor cross-validation statistics for gridding (Figure 6), indicating that their growth anomalies differ greatly from those of surrounding chronologies. The results suggest that the large-scale environmental signal in tree rings in the Pacific Northwest depends strongly on species. Other evidence for such species dependence is the preponderance of ponderosa pine in the final sets of predictors from best-subset regression of annual precipitation against tree-ring data from various species in the Pacific Northwest (Graumlich 1987).

4. Climatological interpretation

The tree-growth "regions" defined by the PCs in Fig. 8 broadly resemble drought regions identified by Karl and Koscielny (1982) in an RPCA of gridded PDSI, 1895–1981. The centers of tree-ring regions and drought regions are listed in Table 2. Of nine drought regions, only the "east north central" is without a tree-ring counterpart. Centers of drought regions and tree-ring regions nearly coincide in Arizona, Georgia, Texas, Montana, and the Northeast. Centers differ considerably in location near the Great Lakes, and in the midwestern and south-central states. For example, the central part of the Arkansas tree-ring region straddles

TABLE 2. Comparison of central locations of tree-ring and Palmer Index rotated PCs.

N_1[a]	Name[b]	Center[c] PDSI	Center,[d] tree	N_2[e]
1	South	Central Texas	Texas	(7)
2	West north central	Eastern Montana	Eastern Montana	(5)
3	Central	Southern Indiana	Northern Indiana	(3)
4	Northwest	Oregon–Washington	Washington	(8)
5	Southwest	Arizona	Arizona	(1)
6	West	Central California	Northern California	(4)
7	Southeast	Georgia	Georgia	(9)
8	East north central	Southern Minnesota	"no good analog"	
9	Northeast	New Hampshire	Vermont–New Hampshire	(2)

[abc] Palmer Index PC, name of drought region, and approximate location of geographical center of region, from Fig. 5 in Karl and Koscielny (1982).
[d] Geographical center of high primary pattern coefficients for rotated tree-ring PCs in Fig. 8.
[e] Tree-ring PC number, from Fig. 8.

the boundary between the central and south drought regions; and the center of the north central drought region (southern Minnesota) is between the Montana and New England tree-ring regions (Fig. 8). Even if tree-ring data were perfect estimators of PDSI, differences in analysis period, data reduction methods (e.g., gridding algorithms), and RPCA methods would cause some differences in locations of identified regions. For example, Cook et al. (1992) found that the number of drought regions from RPCA of tree ring–reconstructed PDSI in the eastern United States differs depending on whether the analysis is on the full period (1700–1972) or the recent period (1895–1972).

Similarities in regions marked by RPCA of PDSI and tree rings could be caused by a common response in the two types of variables to some component of drought. We tested for a drought signal in the tree-ring PCs by computing correlations between the PC scores and July PDSI, 1929–79, averaged over central grid points of the PCs. July or June PDSI has been successfully reconstructed from tree-ring data in widely separate parts of the conterminous United States (Cook and Jacoby 1977; Meko et al. 1980; Cleaveland and Duvick 1992; Stahle and Cleaveland 1988). July PDSI for the 1035 Historical Climate Network (HCN) stations was gridded to the tree-ring grid (Fig. 5) and averaged over grid points before correlation with tree-ring PC scores. PDSI was gridded by the same algorithm (3) used to grid the tree-ring data, except that only the nearest three stations were allowed to enter for each grid point. This restriction avoids possible inhomogeneities caused by the widely varying HCN station density. Gridded PDSI was then averaged over 2–7 central grid points of the tree-ring PCs before correlation with PC scores (solid circles in Fig. 8). Grid points over which to average were selected by trial and error to maximize the correlation with PC scores.

Correlations and the corresponding time series plots for the period 1929–1979 are shown in Fig. 11. Series have been standardized to zero mean and unit standard deviation to facilitate comparison. The strength of the PDSI signal varies greatly over the nine PCs. The signal is strongest in the southwest ($r = 0.86$) and lowest in the coastal Pacific Northwest ($r = 0.14$). Correlations are generally higher in the south and the semiarid west, and exceed 0.7 for regions centered on Arizona, Montana, Arkansas, and Texas. Low-frequency and high-frequency PDSI variations are tracked closely by the tree-ring PC scores in these regions.

The variation in strength of PDSI signal over the nine tree-growth regions has several possible explanations. First, moisture stress is not equally limiting to growth in all regions. Second, differences in the number of chronologies in the search radius around grid points cause differences in the amount of nonclimatic "noise" in the gridded values. Third, gridding masks or damps seasonal climate signals that are species dependent. The gridding cross-validation results discussed previously show that this problem is more severe in the Pacific Northwest and the Northeast than in the Southwest. Fourth, July PDSI cannot be the "best" drought variable for relation to tree growth for every chronology in the network. The precipitation signal in bald cypress from Georgia, for example, is mainly restricted to an April–June window (Stahle and Cleaveland 1992), but the signal in conifers from the Southwest has a significant contribution from fall and winter rainfall (Fritts 1976). Fifth, a simple linear correlation coefficient ignores possible lags in the response of tree growth to climate. The importance of lagged response is suggested by tree-ring studies in which reconstruction accuracy is improved by including lagged predictors (e.g., Stockton and Meko 1983). Lagged response might be especially important in mesic environments, where recurrent drought conditions over several years might be needed to appreciably limit growth. Eastern hemlock, a key species in the northeastern part of our network (Fig. 1), has been found to have a one-year lag in response to June and July temperature anomalies (Cook and Cole 1991).

Because of their high correlation with PDSI, the scores of tree-ring PCs centered on Arizona, Montana, Arkansas, and Texas are useful proxy series for drought. Smoothed PC scores are plotted for the period 1706–

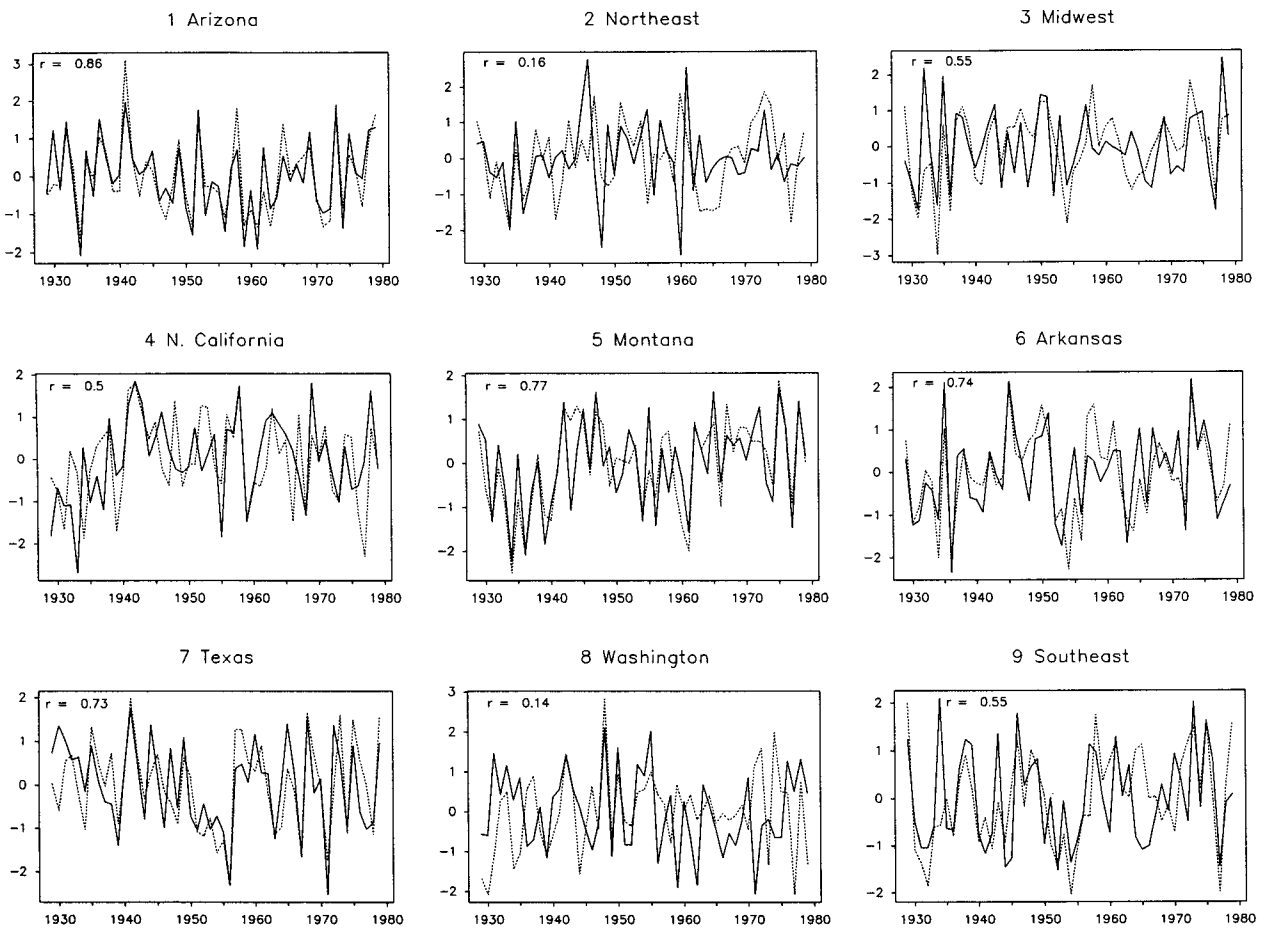

FIG. 11. July Palmer Drought Severity Index and PC scores of tree growth, 1929–79. Series are standardized to zero mean and unit standard deviation. PC scores (solid) are from oblique rotation of gridded tree-ring data (see Figure 8). Drought index (dashed) is averaged over 2–7 grid points with highest pattern coefficients in tree-growth PCs.

1978 in Fig. 12. Horizontal lines at the 0.1 and 0.9 quantiles help to identify periods of extreme drought or wetness. Simultaneous large departures in Fig. 12 mark periods of drought or wetness interregional in extent. Although the largest correlation coefficient between any pair of the four unsmoothed PC-score series, 1705–1979, is only 0.16, several important interregional features are evident. For example, the Arizona and Montana series have a wavelike growth feature with peaks (wet) in the 1830s and early 1900s. The large number of values above the 0.9 quantile in these series indicates that the 1929–78 period on which the quantiles were computed was anomalous in the interior West for its lack of extreme wetness. The Arizona series is characterized by an abrupt increase in importance of low-frequency variation after 1900: the twentieth century is dominated by a downward trend from the early 1900s to the mid-1950s, followed by an upward trend to the end of record.

Tree-growth PCs centered on Arizona, Texas, and Arkansas (PCs 1, 6, and 7 in Fig. 8) are favorably located for inferring occurrence of widespread drought across the southern United States. The smoothed series in Fig. 12 and their unsmoothed counterparts were analyzed to place the drought of the 1950s in a long-term perspective. The 1950s drought has been the subject of several case studies of large-scale drought. Thomas (1962) found that annual precipitation was below normal over large areas of the Southwest for each year from 1952 to 1956, and that the center of drought shifted from one year to another within the seven southwestern states. Borchert (1971) classified the 1950s as a "Southern Plains" drought, with summer rainfall for 1952–55 less than 80% of normal across the South from Texas to Georgia. Namias (1955) used the 1952–54 period for a case study of summertime drought in the continental United States; he attributed the unusual persistence and spatial extent of the drought to the anomalous development and positioning of an upper-level anticyclone over the southern United States.

A simple tree-ring proxy for southern drought is the simultaneous occurrence of low PC scores for PCs 1, 6, and 7. Thresholds for drought in the individual score series were arbitrarily set to the 0.1, 0.2, and 0.3 quantiles, and years in which all three PC scores were below

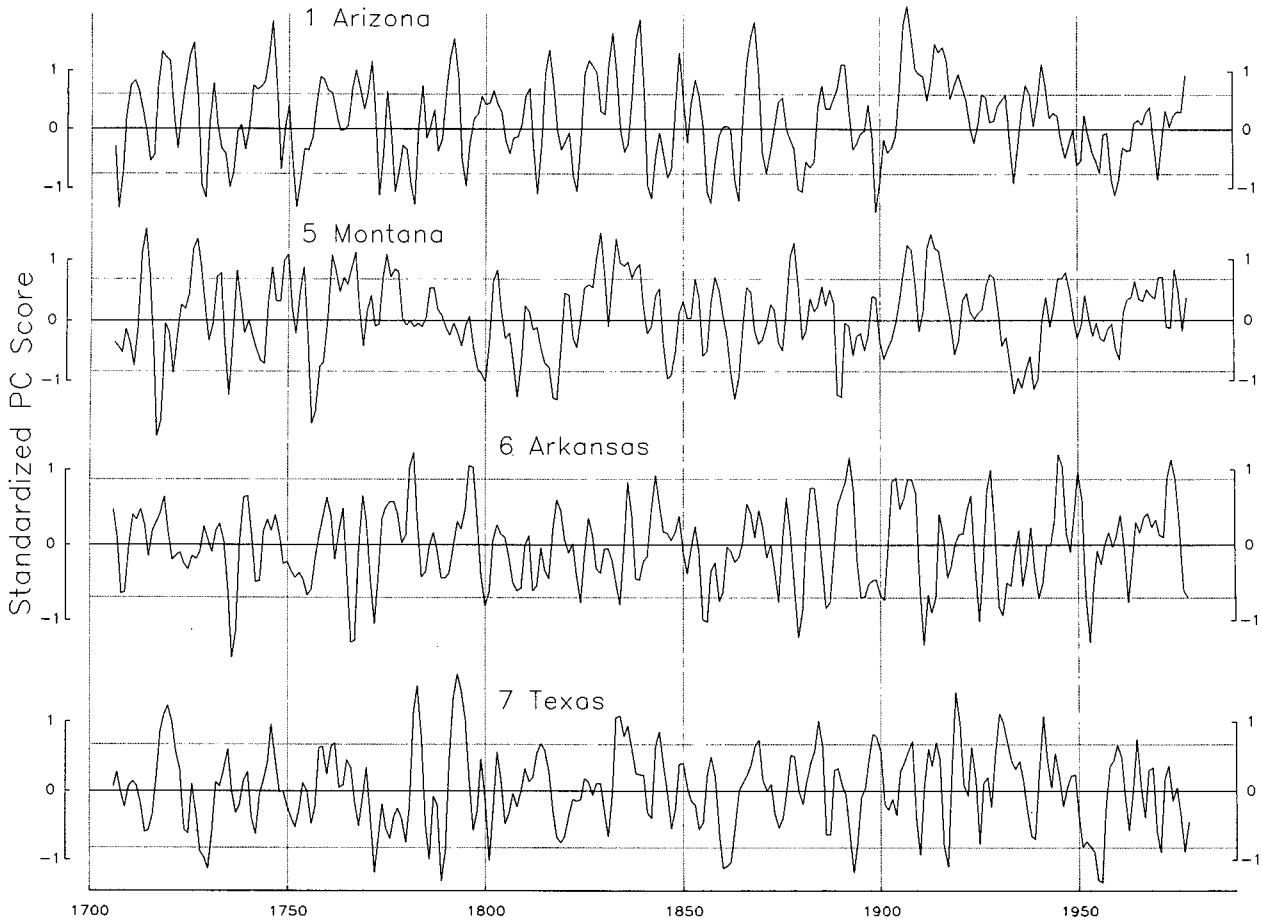

FIG. 12. Smoothed standardized series of PC scores of tree growth, 1705–1979. Each annual series was standardized before smoothing by subtracting the 1929–79 mean and dividing by the 1929–79 standard deviation. The dashed horizontal lines mark the 0.1 and 0.9 quantiles of the smoothed series for the period 1929–1978. Filter weights for smoothing are 0.25, 0.5, 0.25. Smoothing does not decrease correlations with 1929–79 July PDSI appreciably for any region, and increases the correlation from 0.77 to 0.85 for region 5.

each threshold were identified. The analysis was done for both the smoothed series plotted in Fig. 12 and the unsmoothed series. A tabulation using these thresholds indicates that there were no southern droughts at the 0.1 quantile, but several at the 0.2 and 0.3 quantiles. Droughts at the 0.3 quantile are listed below, with asterisks marking those also qualifying at the 0.2 quantile.

Annual	Smoothed
1728	1751
1780	1752
1859	1773
1894	1954
1953*	1956
1956*	1963
1963*	

The 1950s is a prominent feature in the tabulations for both the smoothed and unsmoothed series. At the 0.3 quantile for drought severity, three of the six droughts in the smoothed series and three of the seven droughts in the unsmoothed series were in the period 1953–1963. At the 0.2 quantile, all southern droughts were in the period 1953–1963. The tabulations suggest that the 1950s drought is the extreme event of recurrent widespread drought in the southern United States since 1705.

5. Concluding remarks

Large-scale environmental influences impose a regional coherence on tree growth variations over the United States. For much of the United States outside the Pacific Northwest and New England, our results show that drought is an important influence on this coherence. The signal for July PDSI is strong enough in some parts of the semiarid West that tree rings gridded or averaged over chronologies are accurate drought proxies without conversion to drought estimates by regression modeling to account for species dependence or lag in the growth response to climate. Gridding tree-ring data might be helpful for getting an even sample distribution for large-scale reconstruction of climate in these regions—and elsewhere if all chronologies are the same species. Gridding has the advantage over, say,

sparse sampling of using all available tree-ring data, but the drawback of averaging growth anomalies over species with different seasonal climate signals. Results from cross-validation of gridding and from RPCA on ungridded data indicate that the drawback is greatest in the Pacific Northwest and New England. If tree-ring data from these regions are to be gridded for climate analysis, chronologies should be screened to ensure that they measure the same climate signal. RPCA might be a useful tool for such screening.

The strength of the drought signal that is resolvable from tree rings depends on site coverage, which in this study was limited by the criterion of time coverage through 1979. If this criterion were relaxed to include chronologies collected before 1979, many additional chronologies would be added in the western United States and the drought signal there would probably be strengthened. Ongoing collections throughout temperate North America should also continuously improve the capability to study spatial patterns of drought. Applicability of the network for study of large-scale drought features such as those related to the Southern Oscillation would be improved by extending the network geographically into Mexico and western Canada. The dataset we have compiled is the most widely distributed and densely replicated network of annually resolved proxy climate data yet developed. We intend to submit this tree-ring network to the National Geophysical Data Center at Boulder, Colorado, where the data will be accessible for analyses of the historical patterns, interrelationships, and causes of United States moisture anomalies. The information should be generally useful to climate modelers and others in advancing our knowledge of regional climate variability on the decade-to-century time scale.

Acknowledgments. This research has been supported by National Science Foundation Grant ATM-88-14675. Thomas Swetnam, Donald Graybill, Malcolm Cleaveland, and Paul Sheppard offered helpful comments on the manuscript. Much of the Pacific Northwest part of the network is the result of chronology development by Linda Brubaker and colleagues at the College of Forest Resources, University of Washington. Additional chronologies were generously contributed by Lisa Graumlich, Donald Graybill, Gordon Jacoby, Paul Sheppard, and Thomas Swetnam. Don Myers offered suggestions on geostatistical methods. Gene Willeke and Nathaniel Guttman provided the National Drought Atlas drought indices.

APPENDIX

Equations for Variance Stabilization

This method of variance stabilization is an option in the ARSTAN Fortran computer package for tree-ring standardization (Cook and Holmes 1984).

Assume a site chronology X_t that has already been detrended in mean using conventional procedures (Cook et al. 1990). A trend in variance of X_t implies a trend in the absolute deviations from the mean $d_t = |X_t - \bar{X}_t|$, where $\bar{X}_t$ is the 1700–1979 mean index.

Estimate a trend line $\hat{d}_t$ by fitting d_t to a straight line or modified negative exponential curve

$$\hat{d}_t = At + B$$

$$\hat{d}_t = Ce^{-Dt} + F, \quad (1)$$

where A, B, C, D, and F are coefficients to be estimated, and t is the year.

Scale the absolute deviations d_t by multiplying by the ratio of the mean absolute deviation to the value of the fitted trend line in a given year:

$$d'_t = \left(\frac{\bar{d}_t}{\hat{d}_t}\right) d_t, \quad (2)$$

where $\bar{d}_t$ is the mean absolute deviation for 1700–1979. Restore the original sign of the deviations, and add to the 1700–1979 mean index to get the variance-stabilized chronology

$$X'_t = \bar{X} \pm d'_t. \quad (3)$$

REFERENCES

Bigg, G. R., 1991: Kriging and intraregional rainfall variability in England. *Int. J. Climatol.*, **11**, 663–675.

Borchert, J. R., 1971: The dust bowl in the 1970s. *Ann. Assoc. Amer. Geogr.*, **61**, 1–22.

Chbouki, N., 1991: Spatio-temporal characteristics of drought as inferred from tree-ring data in Morocco. Ph.D. dissertation, University of Arizona, Tucson, Arizona, 243 pp. Available from University of Arizona, Main Library, Tuscon, AZ, 85721.

Cleaveland, M. K., and D. N. Duvick, 1992: Iowa climate reconstructed from tree rings, 1640–1982. *Water Resour. Res.*, **28**, 2607–2615.

Cook, E. R., and G. C. Jacoby, 1977: Tree-ring–drought relationships in the Hudson Valley, New York. *Science*, **198**, 399–401.

——, and K. Peters, 1981: The smoothing spline: A new approach to standardizing forest interior tree-ring width series for dendroclimatic studies. *Tree-Ring Bull.*, **41**, 45–53.

——, and R. L. Holmes, 1984: Program ARSTAN Users Manual. Unpublished manuscript, Lamont-Doherty Earth Observatory, Palisades, New York, 28 pp. Program and manual available from Laboratory of Tree-Ring Research, Building #58, University of Arizona, Tuscon, AZ 85721.

——, and J. Cole, 1991: On predicting the response of forests in eastern North America to future climate change. *Clim. Change*, **19**, 271–282.

——, D. W. Stahle, and M. K. Cleaveland, 1992: Dendroclimatic evidence from eastern North America. *Climate since A.D. 1500*, R. S. Bradley and P. D. Jones, Eds., Routledge, 331–348.

——, K. Briffa, S. Shiyatov, and V. Mazepa, 1990: Tree-ring standardization and growth-trend estimation. *Methods of Dendrochronology: Applications in the Environmental Sciences*, E. R. Cook and L. A. Kairiukstis, Eds., Kluwer Academic, 104–123.

Cropper, J. P., and H. C. Fritts, 1982: Density of tree-ring grids in western North America. *Tree-Ring Bull.*, **42**, 3–9.

Englund, E., and A. Sparks, 1990: *GEO-EAS (Geostatistical Environmental Assessment Software) User's Guide.* Environmental Monitoring Systems Laboratory, Office of Research and Development, U.S. Environmental Protection Agency. 149 pp.

Finkelstein, P. L., 1984: The spatial analysis of acid precipitation data. *J. Climate Appl. Meteor.*, **23**, 52–62.

Fritts, H. C., 1965: Tree-ring evidence for climatic changes in western North America. *Mon. Wea. Rev.*, **93,** 421–443.

——, 1976: *Tree Rings and Climate.* Academic Press, 567 pp.

——, 1991: *Reconstructing Large-Scale Climatic Patterns from Tree-Ring Data: A Diagnostic Analysis.* University of Arizona Press, 286 pp.

——, G. R. Lofgren, and G. A. Gordon, 1979: Variations in climate since 1602 as reconstructed from tree rings. *Quat. Res. N.Y.*, **12,** 18–46.

Graumlich, L. J., 1987: Precipitation variation in the Pacific Northwest (1675–1975) as reconstructed from tree rings. *Ann. Assoc. Amer. Geogr.*, **77,** 19–29.

Harman, H. H., 1967: *Modern Factor Analysis.* The University of Chicago Press. 474 pp.

Isaaks, E. H., and R. M. Srivastava, 1989: *Applied Geostatistics.* Oxford University Press, 561 pp.

Jennrich, R. I., and P. F. Sampson, 1966: Rotation for simple loadings. *Psychometrika,* **31,** 313–323.

Julian, P. R., 1970: An application of rank-order statistics to the joint spatial and temporal variations of meterorological elements. *Mon. Wea. Rev.*, **98,** 142–153.

Karl, T. R., and A. J. Koscielny, 1982: Drought in the United States: 1895–1981. *J. Climatol.*, **2,** 313–329.

——, A. J. Koscielny, and H. F. Diaz, 1982: Potential errors in the application of principal component (eigenvector) analysis to geophysical data. *J. Appl. Meteor.*, **21,** 1183–1186.

——, C. N. Williams, Jr., F. T. Quinlan, and T. A. Boden, 1990. United States historical climatology network (HCN) serial temperature and precipitation data. ORNL/CDIAC-30, NDP-019/R1, Carbon Dioxide Information Analysis Center, Oak Ridge National Lab., 377 pp. Oak Ridge National Laboratory, Attention: CDIAC, Building 1000, P.O. Box 2008, MS-6335, Oak Ridge, TN 37831-9984.

Katz, R. W., 1982: Statistical evaluation of climate experiments with general circulation models: A parametric time series modeling approach. *J. Atmos. Sci.*, **39,** 1446–1455.

Kutzbach, J. E., and P. J. Guetter, 1980: On the design of paleoenvironmental data networks for estimating large-scale patterns of climate. *Quat. Res. N.Y.*, **14,** 169–187.

Langbein, W. B., and J. R. Slack, 1982: Yearly variations in runoff and frequency of dry years for the conterminous United States, 1911–79. U.S. Geol. Survey Open-File Report 82-751, 85 pp. Branch of Distribution, U.S.G.S., Box 25425, Denver Federal Center, Denver, CO 80225.

Meko, D. M., C. W. Stockton, and W. R. Boggess, 1980: A tree-ring reconstruction of drought in southern California. *Water Resour. Bull.*, **16,** 594–600.

Namias, J., 1955: Some meteorological aspects of drought, with special reference to the summers of 1952–1954 over the United States. *Mon. Wea. Rev.*, **83,** 199–205.

O'Lenic, E. A., and R. E. Livezey, 1988: Practical considerations in the use of rotated principal component analysis (RPCA) in diagnostic studies of upper-air height fields. *Mon. Wea. Rev.*, **116,** 1682–1689.

Panofsky, H. A., and G. W. Brier, 1968: *Some Applications of Statistics to Meteorology.* The Pennsylvania State University Press, 224 pp.

Richman, M. B., 1986: Rotation of Principal components. *J. Climatol.*, **6,** 293–335.

Salas, J. D., J. W. Delleur, V. M. Yevjevich, and W. L. Lane, 1980: *Applied Modeling of Hydrologic Time Series.* Water Resources Publications, 484 pp.

Shao, X., 1992: Statistical relationships between tree growth and climate in western North America. Ph.D. dissertation, University of Arizona, Tucson, 195 pp. University of Arizona, Main Library, Tuscon, AZ 85721.

Shiyatov, S., V. Mazepa, and E. Cook, 1990: Correcting for trend in variance due to changing sample size. *Methods of Dendrochronology: Applications in the Environmental Sciences,* E. R. Cook and L. A. Kairiukstis, Eds., Kluwer Academic Publishers, 133–137.

Stahle, D. W., and M. K. Cleaveland, 1988: Texas drought history reconstructed and analyzed from 1698–1980. *J. Climate,* **1,** 59–74.

——, and ——, 1992: Reconstruction and analysis of spring rainfall over the southeastern USA for the past 1000 years. *Bull. Amer. Meteor. Soc.*, **73,** 1947–1961.

Stockton, C. W., and D. M. Meko, 1983: Drought recurrence in the Great Plains as reconstructed from long-term tree-ring records. *J. Clim. Appl. Meteor.*, **22,** 17–29.

Thomas, H. E., 1962: The meteorologic phenomenon of drought in the Southwest. U.S. Geol. Survey Prof. Paper 372A, Washington, Govt. Printing Office, 43 pp.

Wigley, T. M. L., K. R. Briffa, and P. D. Jones, 1984: On the average value of correlated time series, with applications in dendroclimatology and hydrometeorology. *J. Climate Appl. Meteor.*, **23,** 201–213.

Willeke, G. E., N. B. Guttman, and W. O. Thomas, 1991: A national drought atlas for the United States of America. U.S. Geol. Survey Open-file Report 91-244, 45–50. Branch of Distribution, U.S.G.S., Box 25425, Denver Federal Center, Denver, CO 80225.